Monatshefte für Chemie 128, 1189–1199 (1997)

**Monatshefte für Chemie**
**Chemical Monthly**

Printed in Austria

# The Substitution Chemistry of Ru*Cp**(*tmeda*)Cl

**C. Gemel**[1], **A. LaPensée**[1], **K. Mauthner**[1], **K. Mereiter**[2], **R. Schmid**[1], and **K. Kirchner**[1,*]

[1] Institute of Inorganic Chemistry, Technical University of Vienna, A-1060 Vienna, Austria
[2] Institute of Mineralogy, Crystallography, and Structural Chemistry, Technical University of Vienna, A-1060 Vienna, Austria

**Summary.** Halide abstraction from Ru*Cp**(*tmeda*)Cl (**1**, *tmeda* = $Me_2NCH_2CH_2NMe_2$) with $NaBPh_4$ in $CH_2Cl_2$ leads to the formation of the sandwich complex Ru*Cp**($\eta^6$-$C_6H_5BPh_3$) (**2**). In the presence of $CH_3CN$ (1 equiv.) and CO, however, the cationic complexes [Ru*Cp**(*tmeda*)($CH_3CN$)]$^+$ (**3**) and [Ru*Cp**(*tmeda*)(CO)]$^+$ (**5**) are obtained. In $CH_3CN$, *tmeda* is also replaced giving [Ru*Cp**($CH_3CN$)$_3$]$^+$ (**4**). Complex **1** reacts readily with terminal acetylenes HC≡C*R*, the products depending on the nature of *R* (Ph, $SiMe_3$, *n*-Bu, COOEt). Thus, with *R* = Ph the ruthenacyclopentatriene complex Ru*Cp**($\sigma,\sigma'$-$C_4Ph_2H_2$)Cl (**6**), with *R* = $SiMe_3$ the cyclobutadiene complex Ru(*Cp**)($\eta^4$-$C_4H_2$(1,2-$SiMe_3$)$_2$)Cl (**7**), and with *R* = *n*-Bu and COOEt the binuclear complexes (*Cp**)$RuCl_2$($\eta^2$:$\eta^4$-$\mu_2$-$C_4H_2$(1,3-*R*)$_2$)Ru(*Cp**) (**8**, **9**) are obtained. Furthermore, with diethyl maleate in the presence of 1 equiv. of LiCl, **1** transforms into the new anionic complex Li[Ru(*Cp**)($\eta^2$-$C_2H_2$(COOEt)$_2$)$Cl_2$] (**10**). X-ray structures of **2**, **3**, **4**, **7**, and **10** are included.

**Keywords.** Ruthenium half-sandwich complexes; Tetramethylethylenediamine; Ruthenacycles.

### Substitutionsreaktionen von Ru*Cp**(*tmeda*)Cl

**Zusammenfassung.** Chloridabspaltung von Ru*Cp**(*tmeda*)Cl (**1**, *tmeda* = $Me_2NCH_2CH_2NMe_2$) mittels $NaBPh_4$ in $CH_2Cl_2$ führt zur Bildung des Halbsandwich-Komplexes Ru*Cp**($\eta^6$-$C_6H_5BPh_3$) (**2**), während in Gegenwart von $CH_3CN$ oder CO die beiden kationischen Verbindungen [Ru*Cp**(*tmeda*)($CH_3CN$)]$^+$ (**3**) und [Ru*Cp**(*tmeda*)(CO)]$^+$ (**5**) entstehen. In $CH_3CN$ als Lösungsmittel wird sogar *tmeda* unter Bildung von [Ru*Cp**($CH_3CN$)$_3$]$^+$ (**4**) verdrängt. Komplex **1** reagiert sehr leicht mit terminalen Alkinen HC≡C*R*, wobei die Produkte stark von der Natur des Substituenten *R* (Ph, $SiMe_3$, *n*-Bu, COOEt) abhängen. Im Fall von *R* = Ph entsteht der Ruthenacyclopentatrien-Komplex Ru*Cp**($\sigma,\sigma'$-$C_4Ph_2H_2$)Cl (**6**), mit *R* = $SiMe_3$ der Cyclobutadien-Komplex Ru(*Cp**)($\eta^4$-$C_4H_2$(1,2-$SiMe_3$)$_2$)Cl (**7**), und im Fall von *R* = *n*-Bu und COOEt bilden sich die binuklearen Komplexe (*Cp**)$RuCl_2$($\eta^2$:$\eta^4$-$\mu_2$-$C_4H_2$(1,3-*R*)$_2$)Ru(*Cp**) (**8**, **9**). Überdies reagiert **1** mit Maleinsäurediethylester in Gegenwart von LiCl zum neuen anionischen Komplex Li[Ru(*Cp**)($\eta^2$-$C_2H_2$(COOEt)$_2$)$Cl_2$] (**10**). Von **2**, **3**, **4**, **7** und **10** wurden die Kristallstrukturen bestimmt.

## Introduction

The organometallic chemistry of late transition metals has traditionally been associated with low oxidation states. Thus, mainly $\pi$-acceptor ligands requiring at

least some back donation from the metal to bind well have been used such as CO, polyenes, or tertiary phosphines [1]. Compared to this, $\sigma$ donor and $\sigma/\pi$ donor ligands such as amines, alkoxides, or amides are seldom used. In fact, it has been the general belief that in an 18e complex, *i.e.*, with filled *d*-orbitals, bonding between a hard ligand (*e.g.* N, O donors) and the metal is relatively weak [2], especially if lone pairs weaken the metal ligand bond by repulsion of the filled metal orbitals. Amine, amide, and alkoxo complexes of late transition metals should be favored if the metal is in a high formal oxidation state and coordinatively unsaturated. Under this condition the metal will accept more electron density from the heteroatom ligands, particularly from lone pair electron density.

In the present work we report on the chemistry of the electron-rich half-sandwich complex Ru*Cp**(*tmeda*)Cl (**1**) featuring the pure $\sigma$-donor *tmeda* and the $\sigma/\pi$ donor $Cl^-$. *Kölle et al.* have pointed [3] out that this complex is dynamic in solution due to the equilibrium shown in Eq. (1). Also, in the solid state the Ru-Cl bond in **1** is rather weak as apparent from the unsually long Ru-Cl distance of 2.512(1) Å as determined by X-ray crystallography. Thus, **1** may be a useful new precursor for the synthesis of complexes containing the [Ru*Cp**(*tmeda*)]$^+$ or [Ru*Cp**]$^+$ fragments.

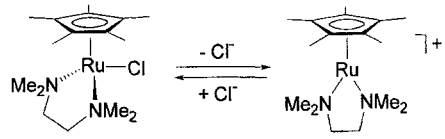


(1)

## Results and Discussion

According to Eq. (1), the chloride ligand in **1** is substitutionally labile and should be easily abstracted by halide scavengers. In fact, treatment of **1** with $NaBPh_4$ in $CH_2Cl_2$ produced a color change from orange to dark violet due to the formation of the cationic 16e intermediate [Ru*Cp**(*tmeda*)]$^+$. This complex has been recently isolated as the $NaBAr'_4$ ($Ar' = 3,5\text{-}C_6H_3(CF_3)_2$) salt [4], being the first 16e complex

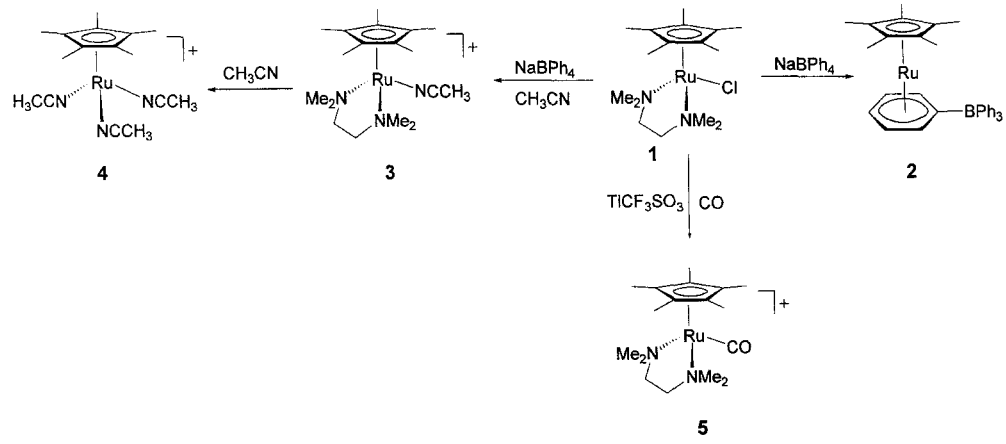


**Scheme 1**

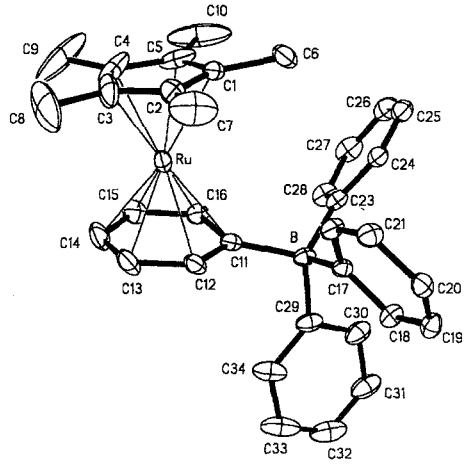


**Fig. 1.** Structural view of Ru*Cp**($\eta^6$-$C_6H_5BPh_3$) (**2**) showing 15% probability thermal ellipsoids; selected bond lengths (Å): Ru-C(1–5)$_{av}$ 2.175(4), Ru-C(11–16)$_{av}$ 2.237(4), C(11)-B 1.656(5), C(17)-B 1.653(4), C(23)-B 1.646(5), C(29)-B 1.653(5)

not stabilized by $\sigma/\pi$-donor ligands. Coordinatively unsaturated half-sandwich ruthenium complexes stabilized by heteroatomic anionic ligands through metal-ligand multiple bonds are known, *e.g.* Ru*Cp**($PR_3$)Cl (*R* = *Cy*, *i*-Pr) and Ru*Cp**($PCy_2CH_2CH_2OMe$)Cl [5, 6]. Within a few minutes, however, the solution became pale yellow; upon work-up, the air-stable 18e sandwich complex Ru*Cp**($\eta^6$-$C_6H_5BPh_3$) (**2**) is obtained (Scheme 1). Characterization of **2** was accomplished by a combination of elemental analysis, $^1$H NMR spectroscopy, and, in addition, by X-ray crystallography (Fig. 1; important bond distances and angles are reported in the caption). Ruthenium is sandwiched between and directly bonded to *Cp** and to one of the phenyl rings of the $BPh_4^-$ group (*cf.* the structure of the analogous complex Ru*Cp*($\eta^6$-$C_6H_5BPh_3$) [7]). The dihedral angle between the planes defined by the *Cp** ring and the $C_6H_5B$ moiety of the $BPh_4^-$ anion is 7.9(3°). The average Ru-C(1–5) and Ru-C(11–16) bond distances are 2.175(4) and 2.237(4) Å, respectively. The $BPh_4^-$ anion shows some distortion from a tetrahedral configuration in that the B atom is *exo*-displaced by 0.30 Å from the plane of the $\eta^6$-bonded phenyl ring.

When the reaction of **1** with $NaBPh_4$ (or $TlCF_3SO_3$) is performed in the presence of $CH_3CN$ (1 equiv.), the intermediate [Ru*Cp**(*tmeda*)]$^+$ is trapped as the cationic complex [Ru*Cp**(*tmeda*)($CH_3CN$)]$^+$ (**3**) (Scheme 1). In neat $CH_3CN$, even *tmeda* is substituted giving the known cationic complex [Ru*Cp**($CH_3CN$)$_3$]$^+$ (**4**) [8, 9]. In the presence of CO instead of $CH_3CN$, the cationic complex [Ru*Cp**(*tmeda*)(CO)]$^+$ (**5**) is formed upon treatment with $TlCF_3SO_3$. The structures of **3** (as the $BPh_4^-$ salt) and **4** (as the $CF_3SO_3^-$ salt) obtained by X-ray crystallography are depicted in Figs. 2 and 3; selected bond distances and angles are given in the captions. Both complexes adopt the usual three-legged piano stool structure. The Ru-N(*tmeda*) distances are 2.235(4) and 2.262(4) Å, respectively, with a N-Ru-N angle of 77.7(1)° (*cf.* the Ru-N distances in **1**: 2.262 (4) and 2.295 (4) Å [3]). The average Ru-*Cp** distance in **3** and **4** is 2.149(4) and 2.148(4) Å, respectively. The Ru-N($CH_3CN$) distances in **3** and **4** are 2.071(4) and 2.104(4) Å, respectively, which is in the range observed for other ruthenium $CH_3CN$ complexes of the same formal oxidation state. While being definitely triclinic ($P\bar{1}$), the crystal structure of **4** stands out by showing a distinct *pseudo*-symmetry with an

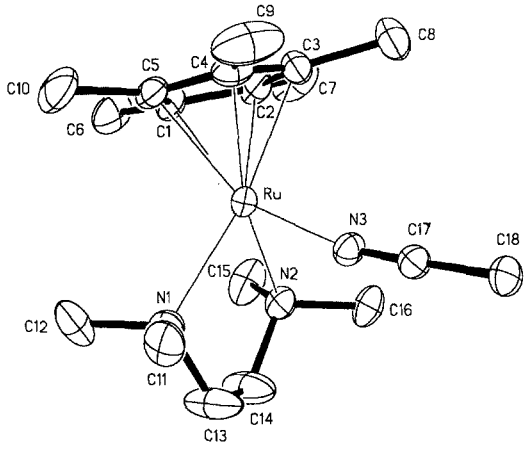


**Fig. 2.** Structural view of [Ru*Cp**(*tmeda*)-$(CH_3CN)]BPh_4 \cdot CH_2Cl_2$ (**3** $\cdot CH_2Cl_2$) showing 20% probability thermal ellipsoids ($BPh_4^-$ and $CH_2Cl_2$ omitted for clarity); selected bond lengths (Å) and angles (°): Ru-C(1–5)$_{av}$ 2.149(5), Ru-N(1) 2.235(4), Ru-N(2) 2.262(4), Ru-N(3) 2.071(4), Ru-N(3)-C(17) 168.6(4), N(3)-C(17)-C(18) 178.2(5), N(1)-Ru-N(2) 77.7(1).

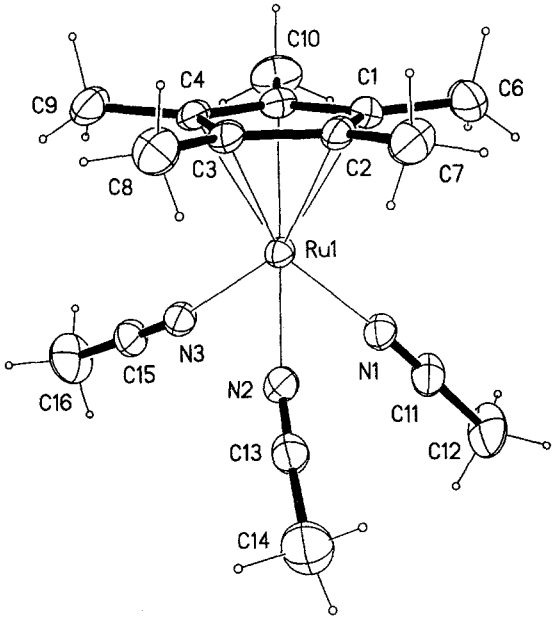


**Fig. 3.** Structural view of [Ru*Cp**-$(CH_3CN)_3]CF_3SO_3$ (**4**) showing 20% probability thermal ellipsoids; only one of the two crystallographically independent complexes is shown; selected bond lengths (Å) and angles (°): Ru(1)-C(1–5)$_{ev}$ 2.153(4), Ru(1)-N(1) 2.101(4), Ru(1)-N(2) 2.105(4), Ru(1)-N(3) 2.106(4), N(1)-Ru(1)-N(2) 85.1(2), N(1)-Ru(1)-N(3) 84.2(1), N(2)-Ru(1)-N(3) 92.3(2)

A-centered *pseudo*-monoclinic cell of the dimensions $a = 19.43$, $b = 11.97$, $c = 19.71$ Å, $\alpha = 89.61$, $\beta = 103.55$, and $\gamma = 87.99°$, and two *pseudo*-dependent ruthenium complexes.

Furthermore, complex **1** was found to react readily with terminal acetylenes HC≡C*R* with the reaction products strongly varying with the substituent *R* (Ph, $SiMe_3$, *n*-Bu, and COOEt). An overview is given in Scheme 2. Thus, with *R* = Ph, *tmeda* is liberated and the mononuclear ruthenacyclopentatriene complex Ru*Cp**($\sigma,\sigma'$-$C_4Ph_4H_2$)Cl (**6**) is formed *via* tail-to-tail dimerization of the acetylene. The analogous complex Ru*Cp*($\sigma,\sigma'$-$C_4Ph_2H_2$)Br is also known [10]. In the $^1$H NMR spectrum of **6**, a sharp singlet is observed for the *Cp** ligand at 1.22 ppm. A signal for two magnetically equivalent hydrogen atoms assignable to the $\beta$-protons of the metallacycle appears at 7.29 ppm. In the $^{13}C\{^1H\}$ NMR spectrum of **6**, the

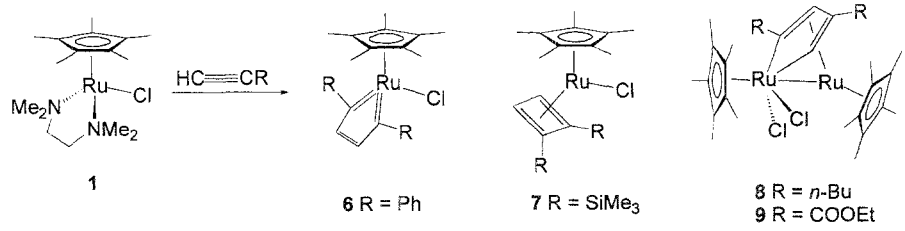


**Scheme 2**

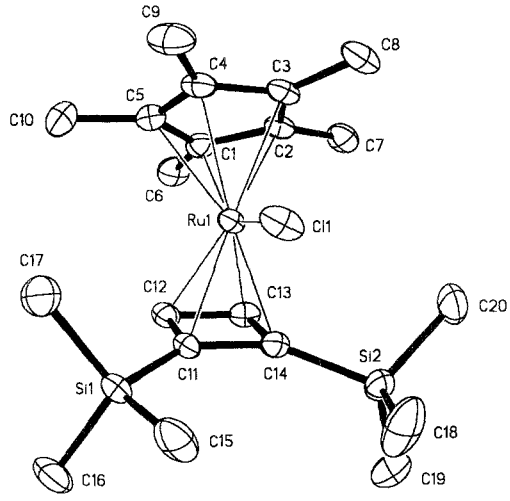


**Fig. 4.** Structural view of Ru(*Cp**)($\eta^4$-$C_4H_2$(1,2-$SiMe_3$)$_2$)Cl (**7**) showing 20% probability thermal ellipsoids; only one of the two crystallographically independent complexes is shown; selected bond lengths (Å): Ru(1)-C(1–5)$_{av}$ 2.253(4), Ru(1)-C(11) 2.153(3), Ru(1)-C(12) 2.138(4), Ru(1)-C(13) 2.132(4), Ru(1)-C(14) 2.145(4), C(11)-C(12) 1.432(5), C(12)-C(13) 1.437(6), C(13)-C(14) 1.447(6), C(11)-(14) 1.528(5), Ru(1)-Cl(1) 2.411(1), C(11)-Si(1) 1.864(4), C(14)-Si(2) 1.851(4)

ruthenacyclopentatriene ring carbons $C_\alpha$ and $C_\beta$ resonate at 263.78 and 158.7 ppm, respectively. The unusual downfield shift of the $C_\alpha$ carbon resonance is in agreement with the formulation of the $C_4Ph_2H_2$ moiety as an unsaturated *bis*-carbene ligand (*cf.* Ru*Cp*($\sigma$,$\sigma'$-$C_4Ph_2H_2$)Br: the resonances of the $C_\alpha$ and $C_\beta$ atoms, respectively, are found at 271.1 and 156.0 ppm [10]).

Treatment of **1** with HC≡C$SiMe_3$ results in the formation of the cylobutadiene complex Ru(*Cp**)($\eta^4$-$C_4H_2$(1,2-$SiMe_3$)$_2$)Cl (**7**) based on elemental analysis and $^1H$ and $^{13}C\{^1H\}$ NMR spectroscopy. In this context, the reaction of [Ru*Cp**Cl]$_4$ with HC≡C$SiMe_3$ should be mentioned [11] in which the $SiMe_3$ substituents of the cyclobutadiene ring were suggested to be in the 1- and 3-position by NMR spectroscopy. Thus, in order to unequivocally establish what isomer is dealt with, the X-ray structure of **7** was determined. Fig. 4 clearly reveals that the two $SiMe_3$ substituents are oriented *cis* to one another, both pointing towards the $Cl^-$ ligand.

There are two crystallographically inequivalent but chemically identical complexes in the unit cell. The dihedral angle between the *Cp** and the cyclobutadiene planes of the two complexes are 38.4 and 39.9°. The bond distances between Ru and the cyclobutadiene are somewhat longer for C(11) and C(14), 2.153(3) and 2.145(4) Å (2.140 and 2.156 Å in complex 2), and shorter for C(12) and C(13), 2.132(4) and 2.138(4) Å (2.128 and 2.132 Å in complex 2), respectively. The average Ru-*Cp** distance is 2.253(4) Å. The Ru(1)-Cl(1) distance is 2.411(1) Å (2.425 Å in complex 2).

When $R = n$-Bu and COOEt, the binuclear complexes (*Cp**)$RuCl_2(\eta^2{:}\eta^4\text{-}\mu_2\text{-}C_4H_2(1,3\text{-}n\text{-}Bu)_2)$Ru(*Cp**) (**8**) and (*Cp**)$RuCl_2(\eta^2{:}\eta^4\text{-}\mu_2\text{-}C_4H_2(1,3\text{-}COOEt_2)$-Ru(*Cp**) (**9**) are obtained in high yields (Scheme 2). Characterization of these complexes was again performed by elemental analysis and $^1H$ and $^{13}C\{^1H\}$ NMR spectroscopy. The $^1H$ NMR spectrum of **8** exhibits resonances for the inequivalent *Cp** ligands (1.74 and 1.35 ppm). The protons of the $\eta^2{:}\eta^4\text{-}\mu_2\text{-}C_4H_2(n\text{-}Bu)_2$ part of the molecule display two sets of doublets centered at 5.30 ($^4J_{HH} = 1.7$ Hz, $\beta$-H) and 8.62 ppm ($^4J_{HH} = 1.7$ Hz, $\alpha$-H). The small $J_{HH}$ coupling constant of 1.7 Hz and the presence of inequivalent substituents are consistent with a 1,3-substitution pattern for the *n*-Bu groups. The $^{13}C\{^1H\}$ NMR sepectrum of **7** exhibits four individual resonances for the unsymmetrically substituted ruthenacylopentadiene ring carbon atoms. The $^1H$ and $^{13}C^1H$ NMR spectra of **9** are similar to those of **8** and are not discussed here. The NMR spectra of **8** and **9** are in agreement with those of (*Cp**)$RuCl_2(\eta^2{:}\eta^4\text{-}\mu_2\text{-}C_4H_4)$Ru(*Cp**) and (*Cp**)$RuCl_2(\eta^2{:}\eta^4\text{-}\mu_2\text{-}C_4H_4(1,3\text{-}SiMe_2)_2)$Ru(*Cp**) described previously [11].

It is known that electron rich complexes of the type Ru*Cp**(*NN*)Cl (*NN* = 2,2′-bipyridine, 1,4-diisopropyl-1,3-diazabutadiene) react readily with olefins bearing electron withdrawing substituents to give the cationic complexes [Ru*Cp**(*NN*)($\eta^2$-olefine)]$^+$ [12, 13]. In the present case, however, the reaction of **1** with dimethyl maleate led to several intractable materials. If, on the other hand, the same reaction is performed in the presence of 1 equiv. of LiCl, an immediate color change from orange to dark red occurrs indicating formation of the new anionic complex $Li[Ru(Cp^*)(\eta^2\text{-}C_2H_2(COOEt)_2)Cl_2]$ (**10**) in essentially quantitative yield (Scheme 3).

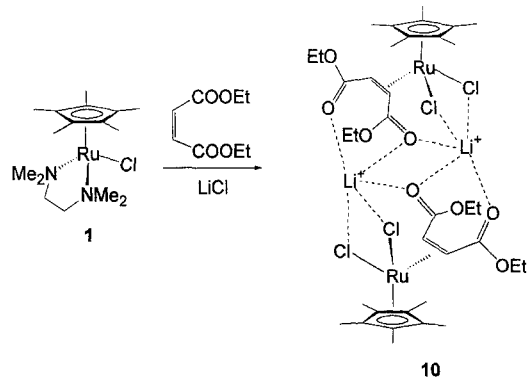


**Scheme 3**

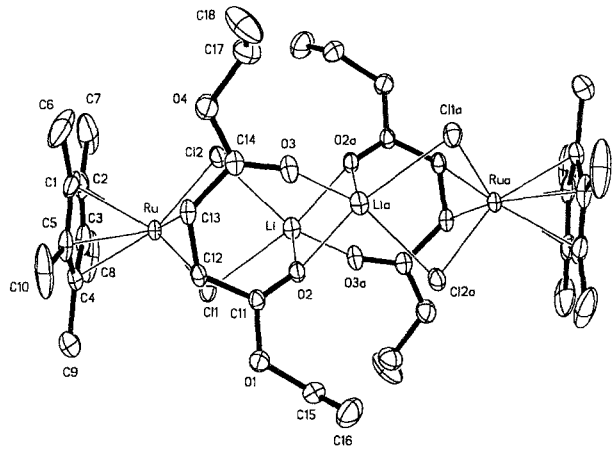


**Fig. 5.** Structural view of Li[Ru(*Cp**)($\eta^2$-$C_2H_2(COOEt)_2$)$Cl_2$] (**10**) showing 20% probability thermal ellipsoids; selected bond lengths (Å) and angles (°): Ru-C(1) 2.173(2), Ru-C(2) 2.256(2), Ru-C(3) 2.240(2), Ru-C(4) 2.168(2), Ru-C(5) 2.161(2), Ru-C(12) 2.166(2), Ru-C(13) 2.144(2), Ru-Cl(1) 2.446(1), Ru-Cl(2) 2.424(1), Li-Cl(1) 2.565(4), Li-Cl(2) 2.452(4), Li-O(2) 1.981(4), Li-O(2a) 2.140(4), Li-O(3a) 1.967(4), C(11)-O(2) 1.215(2), C(14)-O(3) 1.210(2), Cl(1)-Ru-Cl(2) 83.33(3)

Characterization was again accomplished by elemental analysis, and $^1H$ and $^{13}C\{^1H\}$ NMR spectroscopy. The resonances of the vinylic hydrogen and carbon atoms of **10** are shifted upfield to 3.49 and 48.4 ppm compared to 6.21 and 130.0 ppm, respectively, in the free ligand (*cf.* the corresponding resonances in the related complex [Ru*Cp**(2,2-bipyridine)($\eta^2$-$C_2H_2(COOEt)_2$)]$PF_6$ found at 3.60 and 54.3 ppm [12]). Therefore, strong $\pi$-backbonding from the ruthenium center to the alkyne is indicated. Noteworthy, the structure of **10** shown in Fig. 5 is dimeric. Thus, two [Ru*Cp**($\eta^2$-$C_2H_2(COOEt)_2$)$Cl_2$]$^-$ moieties which adopt a piano-stool conformation are connected *via* two $Li^+$ cations to form the neutral complex $Li_2$[Ru*Cp**($\eta^2$-$C_2H_2(COOEt)_2$)$Cl_2$]$_2$ with point symmetry $\bar{1}$. Li exhibits an uncommon tetragonal pyramidal coordination figure with Cl(1), Cl(2), O(2a), and O(3a) forming the square base and O(2) the apex. Two of these units share a common edge. The C(12)–C(13) bond distance of the $\eta^2$-coordinated diethyl maleate is longer (1.417(3) Å) than that in the free olefine (*ca.* 1.34 Å) as a result of $\pi$-backbonding in the $\pi$* orbital of diethyl maleate. The Ru-Cl(1) and Ru-Cl(2) distances are 2.565(4) and 2.452(4) Å, respectively. The two $Cl^-$ ligands exert a distortion on the *Cp** ligand as apparent from the long Ru-C(2) and Ru-C(3) distances (2.248 Å) as compared with the Ru-C(1), Ru-C(4), and Ru-C(5) distances (2.167 Å).

## Experimental

*General Information*

All manipulations were performed under an inert atmosphere of argon using *Schlenk* techniques. All chemicals were standard reagent grade and used without further purification. The solvents were

purified according to standard procedures [14]. The deuterated solvents were purchased from Aldrich and dried over 4 Å molecular sieves. Ru*Cp*(tmeda)*Cl (**1**) was prepared according to the literature [3]. $^{1}H$ and $^{13}C\{^{1}H\}$ NMR spectra were recorded on a Bruker AC-250 spectrometer operating at 250.13 and 62.86 MHz, respectively, and were referenced to internal $SiMe_4$. Microanalyses were done by Microanalytical Laboratories, University of Vienna.

*RuCp*($\eta^2$-$C_6H_5BPh_3$)* (**2**)

A solution of **1** (103 mg, 0.265 mmol) and $NaBPh_4$ (91 mg, 0.265 mmol) in $CH_2Cl_2$ (5 ml) was stirred for 2 h at room temperature. Insoluble materials were removed by filtration, and the solvent was removed *in vacuo*. The crude product was dissolved in $CH_2Cl_2$; addition of $Et_2O$ afforded a precipitate of analytically pure **2**.

Yield: 124 mg (84 %); $C_{34}H_{35}BRu$ (555.54); calc.: C 73.51, H 6.35; found: C 73.24, H 6.17; $^{1}H$ NMR ($\delta$, $CDCl_3$, 20°C): 7.49 (m, 6H), 7.09 (m, 6H), 6.97 (m, 3H), 5.58 (m, 2H), 5.10 (m, 2H), 4.93 (m, 1H), 1.74 (s, 15H, $C_5Me_5$) ppm.

*[RuCp*(tmeda)($CH_3CN$)]$BPh_4$* (**3**)

To a solution of **1** (52 mg, 0.134 mmol) in $CH_2Cl_2$ (5 ml) $NaBPh_4$ (46 mg, 0.134 mmol) and $CH_3CN$ (5.5 mg, 0.134 mmol) were added, and the mixture was stirred for 2 h. The volume of the solution was then reduced to about 1 ml; the product precipitated upon addition of diethyl ether.

Yield: 75 mg (78 %); $C_{42}H_{54}BN_3Ru$ (712.80); calc.: C 70.77, H 7.64, N 5.90; found: C 70.92, H 7.78, N 5.46; $^{1}H$ NMR ($\delta$, $CDCl_3$, 20°C): 7.69 (m, 20H), 7.53 (m, 10H), 2.65 (s, 6H), 2.15 (s, 4H), 1.59 (s, 3H), 1.41 (s, 15H, $C_5Me_5$) ppm.

*[RuCp*($CH_3CN$)$_3$]$CF_3SO_3$* (**4**)

A solution of **1** (62 mg, 0.160 mmol) in $CH_3CN$ was treated with 1 equiv. of $TlCF_3SO_3$, and the mixture was stirred for 10 h at 50 °C. After removal of the solvent, the crude product was dissolved in $CH_3CN$, and insoluble materials were removed by filtration. Upon addition of diethyl ether, a yellow precipiate was obtained which was collected on a glass frit, washed with dimethyl ether, and dried under vaccum.

Yield: 64 mg (79%); $^{1}H$ and $^{13}C\{^{1}H\}$ NMR spectra were in agreement with reported values [8, 9].

*[RuCp*(tmeda)(CO)]$CF_3SO_3$* (**5**)

To a solution of **1** (58 mg, 0.149 mmol) in MeOH (5 ml), $TlCF_3SO_3$ (1 equiv.) was added and stirred for 10 min. After that time, the solution was purged with CO for 1 min. The solvent was removed under vacuum, and the crude product was dissolved in $CH_2Cl_2$. Insoluble materials were removed by filtration; the product precipitated upon addition of diethyl ether.

Yield: 65 mg (82%); $C_{18}H_{31}F_3N_2O_4SRu$ (529.58); calc.: C 40.83, H 5.90, N 5.29; found: C 41.08, H 6.04, N 4.93; $^{1}H$ NMR ($\delta$, $CDCl_3$, 20°C): 3.02–2.91 (m, 2H), 2.85 (s, 3H), 2.78–2.67 (m, 2H), 1.68 (s, 15H, $C_5Me_5$) ppm; $^{13}C$ NMR ($\delta$, $CDCl_3$, 20°C): 205.2 (CO), 94.0 ($C_5Me_5$), 64.7, 60.3, 56.7, 11.0 ($C_5Me_5$) ppm.

*RuCp*($\sigma,\sigma'$-$C_4H_2Ph_2$)Cl* (**6**)

To a solution of **1** (95 mg, 0.245 mmol) in $Et_2O$ (5 ml), HC≡CPh (125 mg, 1.23 mmol) was added, and the mixture was stirred overnight at room temperature. The solvent was removed *in vacuo* and the residue was washed with *n*-hexane.

Yield: 65 mg (56%); $C_{26}H_{27}ClRu$ (476.03); calc.: C 65.60, H 5.72; found: C 65.74, H 5.68; $^1H$ NMR ($\delta$, $CDCl_3$, 20°C): 7.59 (m, 2H), 7.29 (s, 2H), 7.22–7.10 (m, 8H), 1.22 (s, 15H, $C_5Me_5$) ppm; $^{13}C$ NMR ($\delta$, $CDCl_3$, 20°C): 263.8, 158.7, 155.2, 129.2, 128.7, 124.3, 106.3 ($C_5Me_5$), 10.11 ($C_5Me_5$) ppm.

*RuCp*($\eta^4$-$C_4H_2$(1,2-$SiMe_3$)$_2$)Cl* (**7**)

**7** was prepared analogously to **6** using HC≡CSiMe$_3$ instead of HC≡CPh.

Yield: 78%; $C_{20}H_{35}ClRuSi_2$ (468.20); calc.: C 51.31, H 7.54; found: C 51.38, H 7.34; $^1H$ NMR ($\delta$, $CDCl_3$, 20°C): 3.90 (s, 2H), 1.75 (s, 15H, $C_5Me_5$), 0.05 ($SiMe_3$) ppm; $^{13}C$ NMR ($\delta$, $CDCl_3$, 20°C): 99.3 ($C_5Me_5$), 85.1, 78.6, 11.6 ($C_5Me_5$), 1.4 ($SiMe_3$) ppm.

*(Cp*)RuCl$_2$($\eta^2$:$\eta^4$-$\mu_2$-$C_4H_2$(1,3-n-Bu)$_2$)Ru(Cp*)* (**8**)

**8** was prepared analogously to **6** using HC≡CBu$^n$ instead of HC≡CPh.

Yield: 73%; $C_{32}H_{50}Cl_2Ru_2$ (707.80); calc.: C 54.30, H 6.12; found: C 54.12, H 6.28; $^1H$ NMR ($\delta$, $CDCl_3$, 20°C): 8.62 (d, 1H, $J = 1.7$ Hz), 5.30 (d, 1H, $J = 1.7$ Hz), 1.74 (s, 15H, $C_5Me_5$), 1.35 (s, 15H, *Cp**), 2.5–0.8 (m, 18H) ppm $^{13}C$ NMR ($\delta$, $CDCl_3$, 20°C): 185.7, 166.1, 110.0, 104.0, 94.0, 93.3, 43.1, 34.1, 33.0, 32.1, 23.9, 23.8, 15.1, 14.8, 11.2 ($C_5Me_5$), 10.0 ($C_5Me_5$) ppm.

*(Cp*)RuCl$_2$($\eta^2$:$\eta^4$-$\mu_2$-$C_4H_2$(1,3-COOEt)$_2$)Ru(Cp*)* (**9**)

**9** was prepared analogously to **6** using HC≡CCOOEt instead of HC≡CPh.

Yield: 74%; $C_{30}H_{42}Cl_2O_4Ru_2$ (739.71); calc.: C 48.71, H 5.72; found: C 48.96, H 6.03; $^1H$ NMR ($\delta$, $CDCl_3$, 20°C): 9.3 (d, 1H, $J = 1.9$ Hz), 6.33 (d, 1H, $J = 1.9$ Hz), 4.4–4.1 (m, 4H, $OCH_2CH_3$), 1.67 (s, 15H, $C_5Me_5$), 1.44 (s, 15H, $C_5Me_5$), 1.34 (t, 6H, $J = 7.2$ Hz, $OCH_2CH_3$) ppm; $^{13}C$ NMR ($\delta$, $CDCl_3$, 20°C): 203.2, 174.8, 170.5, 168.1, 155.6, 107.0, 101.1, 97.1, 61.5, 61.2, 15.2, 15.1, 10.4, 10.3 ppm.

*Li[Ru(Cp*)($\eta^2$-$C_2H_2$(COOEt)$_2$)Cl$_2$]* (**10**)

A solution of **1** (112 mg, 0.289 mmol) and LiCl (61 mg, 1.44 mmol) in *THF* (5 ml) was treated with diethyl maleate (50 mg, 0.289 mmol), whereupon an immediate color change from orange to dark red occurred. The solution was stirred for 2 h at room temperature, and the solvent was removed *in vacuo*. The residue was dissolved in $Et_2O$, insoluble materials were removed by filtration, and the solvent was again removed *in vacuo*. The resulting solid was collected on a glass frit and washed with *n*-hexane.

Yield: 124 mg (81%); $C_{18}H_{27}Cl_2LiO_4Ru$ (486.33); calc.: C 44.46, H 5.60; found: C 44.32, H 5.67; $^1H$ NMR ($\delta$, acetone-$d_6$, 20°C): 4.25–3.90 (m, 4H, $OCH_2CH_3$), 3.49 (s, 2H), 1.39 (s, 15H, $C_5Me_5$), 1.22 (t, 6H, $J = 7.3$ Hz, $OCH_2CH_3$) ppm; $^{13}C$ NMR ($\delta$, acetone-$d_6$, 20°C): 179.5, 131.4, 96.6 ($C_5Me_5$), 61.1, 48.4, 15.8, 9.1 ($C_5Me_5$) ppm.

*X-ray structure Determination of* **2**, **3** · $CH_2Cl_2$, **4**, **7**, *and* **10**

Crystal data and experimental details are given in Table 1. X-ray data for **2**, **3** · $CH_2Cl_2$, and **4** were collected on a Philips PW1100 four-circle diffractometer using graphite monochromated MoK$\alpha$ ($\lambda = 0.71073$ Å) radiation and the $\Theta$–$2\Theta$ scan technique. For **7** and **10**, a Siemens Smart CCD area detector diffractometer, graphite monochromated MoK$\alpha$ radiation, a nominal crystal-to-detector distance of 3.85 cm, and 0.3° $\omega$-scan frames were used. Corrections for *Lorentz* and polarization effects, and, where necessary, for absorption were applied. Structures **2** and **3** · $CH_2Cl_2$ were solved

**Table 1.** Crystallographic data

| | **2** | **3** · $CH_2Cl_2$ | **4** | **7** | **10** |
|---|---|---|---|---|---|
| Formula | $C_{34}H_{35}BRu$ | $C_{43}H_{56}BCl_2N_3Ru$ | $C_{17}H_{24}F_3N_3O_3RuS$ | $C_{20}H_{35}ClRuSi_2$ | $C_{18}H_{27}Cl_2LiO_4Ru$ |
| Fw | 555.50 | 797.69 | 508.52 | 468.18 | 486.31 |
| Cryst.size (mm) | 0.40×0.45×0.60 | 0.10×0.36×0.82 | 0.27×0.28×0.55 | 0.56×0.34×0.30 | 0.44×0.40×0.36 |
| Space group | P $\bar{1}$ (No. 2) | P $\bar{1}$ (No. 2) | P $\bar{1}$ (No. 2) | Pccn (No. 56) | $P2_1/n$ (No. 14) |
| $a$ (Å) | 11.067(3) | 11.653(3) | 11.494(3) | 21.620(4) | 9.508(2) |
| $b$ (Å) | 11.235(4) | 11.699(3) | 11.564(2) | 29.914(6) | 14.965(3) |
| $c$ (Å) | 12.367(4) | 16.607(5) | 19.426(2) | 14.942(3) | 15.601(3) |
| $\alpha$ (°) | 81.42(2) | 73.50(2) | 79.54(1) | | |
| $\beta$ (°) | 67.86(2) | 87.13(2) | 77.34(1) | | 107.38(1) |
| $\gamma$ (°) | 88.39(2) | 77.14(2) | 62.56(1) | | |
| $V$ (Å$^3$) | 1407.7(8) | 2116(1) | 2226.1(7) | 9664(2) | 2118.5(7) |
| $Z$ | 2 | 2 | 4 | 16 | 4 |
| $\rho_{calc}$ (g · cm$^{-3}$) | 1.311 | 1.252 | 1.517 | 1.287 | 1.525 |
| $T$ (K) | 295 | 295 | 297 | 298 | 298 |
| $\mu$ (mm$^{-1}$), (MoK$\alpha$) | 0.577 | 0.528 | 0.843 | 0.859 | 1.011 |
| Absorption corr. | none | analytical | none | empirical | empirical |
| Transmiss. fact. min/max | | 0.84/0.95 | | 0.61/0.93 | 0.73/0.93 |
| $\theta_{max}$ (°) | 25 | 23 | 25 | 25 | 30 |
| Index ranges | $-13 \le h \le 13$ | $0 \le h \le 12$ | $-13 \le h \le 13$ | $-30 \le h \le 27$ | $-13 \le h \le 12$ |
| | $0 \le k \le 13$ | $-12 \le k \le 12$ | $-13 \le k \le 13$ | $-32 \le k \le 42$ | $-15 \le k \le 20$ |
| | $-14 \le l \le 14$ | $-18 \le l \le 18$ | $0 \le l \le 23$ | $-21 \le l \le 20$ | $-20 \le l \le 21$ |
| No. of rflns.measd. | 4955 | 5869 | 7859 | 50483 | 16765 |
| No. of unique rflns. | 4955 | 5869 | 7859 | 8449 | 6071 |
| No. of rflns. F > 4 $\sigma(F)$ | 4404 | 4755 | 6146 | 7184 | 5288 |
| No. of params. | 325 | 454 | 526 | 467 | 244 |
| $R(F)$ ($F > 4\sigma(F)$) | 0.036 | 0.042 | 0.040 | 0.040 | 0.028 |
| $R(F)$ (all data) | 0.042 | 0.060 | 0.057 | 0.051 | 0.035 |
| $wR(F^2)$ (all data) | 0.096 | 0.100 | 0.101 | 0.079 | 0.073 |
| Diff.Four.peaks min/max (eÅ$^{-3}$) | −0.47/0.48 | −0.40/0.43 | −0.66/0.78 | −0.32/0.42 | −0.48/0.40 |

$R(F) = \Sigma||F_o| - |F_c||/\Sigma|F_o|, wR(F^2) = [\Sigma(w(F_o^2 - F_c^2)^2)/\Sigma(w(F_o^2)^2)]^{\frac{1}{2}}$

by *Patterson* methods, and structures **4**, **7**, and **10** by direct methods [15]. All non-hydrogen atoms were refined anisotropically, and hydrogen atoms were included in idealized positions [16]. The structures were refined against $F^2$. Additional material to the structure determination may be ordered from *Fachinformationszentrum Karlsruhe, Gesellschaft für wissenschaftlich-technische Information mbH, D-76344 Eggenstein-Leopoldshafen, Federal Republic of Germany*, referring to the deposition numbers CSD 407058, 407057, 407228, 407059, and 407060, the names of the authors, and the citation of the present paper.

## Acknowledgements

Financial support by the *Fonds zur Förderung der wissenschaftlichen Forschung* is gratefully acknowledged (Project No. 11896).

## References

[1] Crabtree RH (1996) The Organometallic Chemistry of the Transition Metals, 2nd edn. Wiley, New York
[2] Joslin FL, Pontier MP, Mague JT, Roundhill DM (1991) Organometallics **10**: 2781
[3] Wang MH, Englert U, Koelle U (1993) J Organomet Chem **453**: 127
[4] Gemel C, Mereiter K, Schmid R, Kirchner K, Organometallics (in press)
[5] Campion BK, Heyn RH, Tilley DD (1988) J Chem Soc Chem Commun 278
[6] Lindner E, Haustein M, Mayer HA, Gierling K, Fawzi R, Steinmann M (1995) Organometallics **14**: 2246
[7] Kruger GJ, du Preez AL, Haines RJ (1974) J Chem Soc Dalton Trans 1302
[8] McNair AM, Boyd DC, Mann KR (1986) Organometallics **5**: 303
[9] Fagan PJ, Ward MD, Calabrese JC (1989) J Am Chem Soc **111**: 1698
[10] Albers MO, de Waal DJA, Liles DC, Robinson DJ, Singleton E, Wiege MB (1986) J Chem Soc Chem Commun 1680
[11] Campion BK, Heyn RH, Tilley DD (1990) Organometallics **9**: 1106
[12] Balavoine GGA, Boyer T, Livage C (1992) Organometallics **11**: 456
[13] de Klerk-Engels B, Delis JGP, Vrieze K, Goubitz K, Fraanje J (1994) Organometallics **13**: 3269
[14] Perrin DD, Armarego WLF (1988) Purification of Laboratory Chemicals, 3rd edn. Pergamon, New York
[15] Sheldrick GM (1986) SHELXS86: Program for the Solution of Crystal Structures. University of Göttingen, Germany
[16] Sheldrick GM (1993) SHELXL93: Program for Crystal Structure Refinement. University of Göttingen, Germany

*Received July 11, 1997. Accepted August 25, 1997*